TWO-DIMENSIONAL MODELING OF ION IMPLANTATION

G. Hobler, E. Langer, S. Selberherr

Institut fuer Allgemeine Elektrotechnik und Elektronik
Technische Universitaet Wien
Gusshausstrasse 27, A-1040 Wien, AUSTRIA

ABSTRACT: We present a two-dimensional model of ion implantation which accounts for position dependent lateral moments. The lateral standard deviation and the lateral kurtosis as a function of depth have been calculated by two-dimensional Monte Carlo simulations for boron, phosphorus, arsenic and antimony in silicon for energies in the range of 10 to 300 keV. The lateral moments as a function of depth and energy as well as the vertical moments as a function of energy have been fitted by simple formulae. We specify a modification of the Gaussian distribution function in order to include the lateral kurtosis with an analytical expression.

1. INTRODUCTION

For the purpose of describing ion implantation profiles, methods based on distribution functions together with spatial moments are now being used for more than 20 years. The principle of these methods is to assume a functional type for the distribution function and to calculate its free parameters from its spatial moments. These moments may be obtained either by experiment or by theory. For a long time only the first two moments, i.e. the mean projected range and the projected range straggling (the standard deviation), could be specified [1], and so the only reasonable distribution function was the Gaussian function. Although this oldest model is still freqently used for sake of simplicity or for lack of higher moments, it is well established today, that for a realistic description of one-dimensional profiles 4 moments must be taken into account [2]. For this purpose the Pearson IV distribution is commonly used, which was introduced by Hofker in 1975 [3].

The first model including lateral spread was presented by Furukawa in 1972 [4]. It is based on the statistical distribution function for one ion, i.e. the response to a

punctiform beam. By a convolution of this distribution function he obtained the distribution under an infinitely steep and infinitely high mask edge. Later this model was extended to the case of arbitrarily shaped mask edges by Runge [5], and further models were developed to account for different stopping powers of mask and bulk material [2],[6].

In this paper we shall give a sophisticated model for the statistical distribution function of one ion. We denote it $f(z,x)$, with z the vertical coordinate (perpendicular to the surface) and x the lateral coordinate. z=x=0 is the point of entrance of the ion. Furukawa and still Runge used a two-dimensional Gaussian function for $f(z,x)$, which may be written $f(z,x)=\mathrm{gauss}(z)\cdot\mathrm{gauss}(x)$. This approach has been refined by Ryssel [7] to $f(z,x)=f_{vert}(z)\cdot\mathrm{gauss}(x)$, with $f_{vert}(z)$ a proper one-dimensional distribution function. Using a Pearson IV function, today's-standard model reads

$$f(z,x) = \mathrm{pears}(z)\cdot\mathrm{gauss}(x) \quad . \tag{1}$$

The major limitation of this description is that it ignores any correlation between the vertical (z) and the

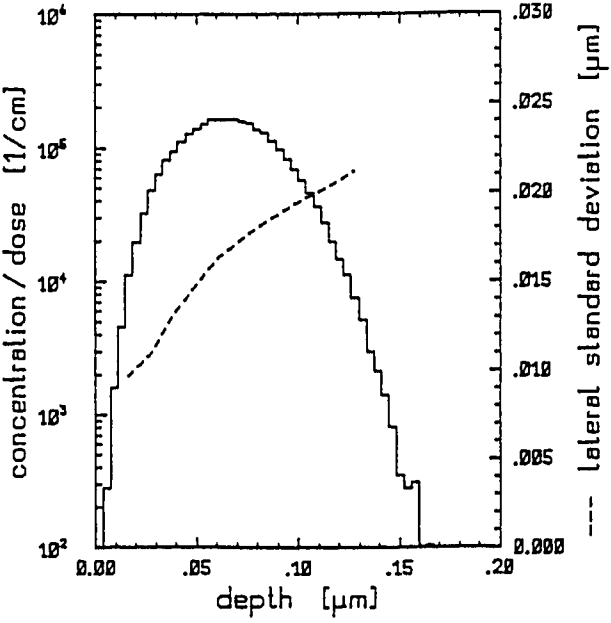

Fig.1: Depth dependence of the lateral standard deviation for As in Si (100 keV)

lateral (x) coordinate, or to say it in more simple words, that the lateral standard deviation is assumed to be independent of the depth. Furthermore, assuming a Gaussian distribution, no higher moments are taken into account. Our Monte Carlo simulations indicate that these assumptions are not true. In Fig.1 and Fig.2 the lateral standard deviation and the lateral kurtosis are shown, respectively, as a function of depth for the case of a 100 keV implantation of arsenic into silicon (dashed lines). As a reference the vertical distribution function (histogram) is also depicted.

The impact on the distribution under a vertical mask edge is shown in Fig.3 and Fig.4. The standard model (Fig.3) is compared to the results of our Monte Carlo simulation (Fig.4) of a 200 keV boron implantation into silicon. This example was chosen because boron has a very large lateral standard deviation. One can see that the classical distribution extends too much below the mask at the maximum concentration of the vertical profile and not enough at regions closer to the surface. The reason for this is that the lateral standard deviation decreases towards the bulk (see Fig.7; this is in contrast to the arsenic implantation of Fig.1).

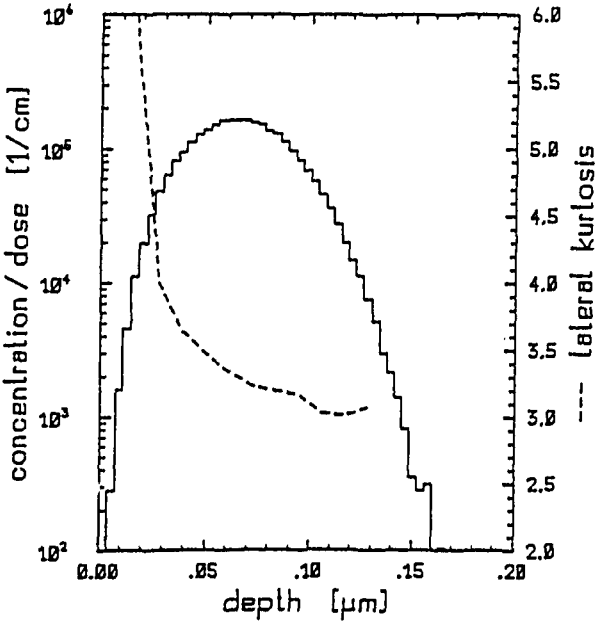

Fig.2: Depth dependence of the lateral kurtosis for As in Si (100 keV)

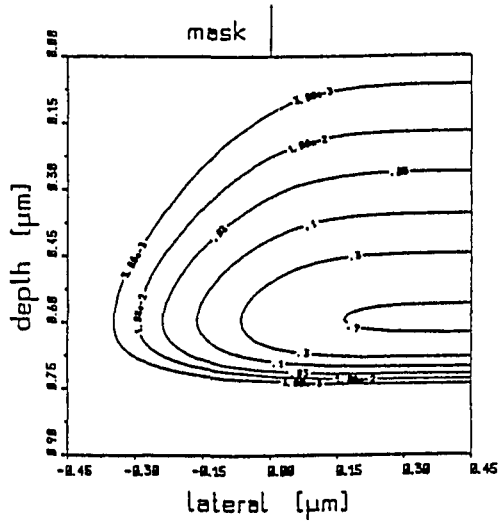

B: 200 keV (Pearson*Gauss)

Fig.3

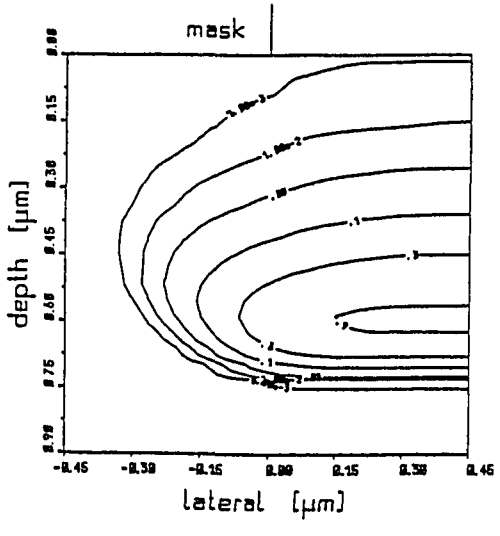

B: 200 keV (Monte-Carlo)

Fig.4

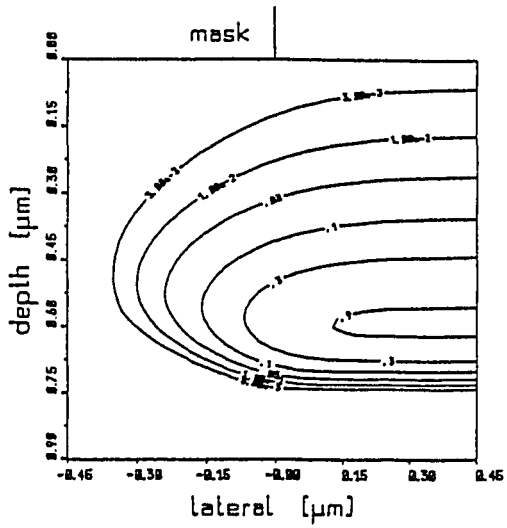

B: 200 keV $\sigma_x(z)$, β_x=3

Fig.5

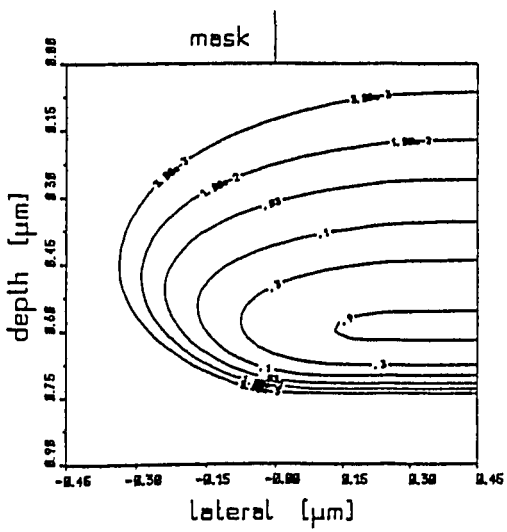

B: 200 keV $\sigma_x(z)$, $\beta_x(z)$

Fig.6

The statistical distribution function for one ion may generally be written

$$f(z,x) = f_{vert}(z) \cdot f_{lat}(x,z) \quad . \tag{2}$$

$f_{lat}(x,z)$ is seen here as a function of x with parameters that depend on the lateral moments, which in turn are functions of the depth (z). In Chapter 4 we shall specify $f_{lat}(x,z)$ as a function of lateral standard deviation σ_x and lateral kurtosis β_x. In Chapter 3 the functions $\sigma_x(z,E)$ and $\beta_x(z,E)$ will be given (E denoting the implantation energy) for the case of boron, phosphorus, arsenic and antimony implantations into silicon in the range of 10 to 300 keV. These were obtained by fitting the results of our Monte Carlo simulations. Also enclosed in Chapter 3 are fitting formulae for the vertical moments as a function of energy. Special features of our Monte Carlo code are briefly outlined in Chapter 2.

2. DETAILS OF THE MONTE CARLO SIMULATION

As with other Monte Carlo codes for the simulation of ion implantation, our code evaluates a large number of ion trajectories in an amorphous target. After entering the solid, the ions undergo collisions with target atoms (nuclei), which cause slowing down and deflection. Additional slowing down is performed by interaction with target electrons. We use the Moliere potential to evaluate nuclear collisions and the Lindhard-Scharff formula to calculate electronic energy loss. These physical fundamentals are identical to those of Biersack's program "TRIM" and are reported in ref. [8]. The correction factor of the electronic stopping formula is chosen 1.5 for boron, 1.3 for phosphorus and 1 else. Recently this approach to the basic physics has been improved by Ziegler, Biersack and Littmark [9] (also reported in [2]).

Our code has some special features in order to increase computer time efficiency. First, the most time consuming part, the evaluation of nuclear collisions, is replaced by linear interpolation in two precomputed tables, which provide the scattering angle and the nuclear energy loss, respectively, as a function of impact parameter and energy. Secondly, we use a special technique to calculate profiles for many different implantation energies simultaneously. And finally we make use of a relationship between the k-th lateral moment $m_k(x)=1/N\cdot\Sigma x_i^k$ and the k-th radial moment $m_k(r)=1/N\cdot\Sigma r_i^k$, $r_i=(x_i^2+y_i^2)^{1/2}$, to reduce statistical fluctuations.

$$m_k(x) = \frac{1}{2}\cdot\frac{3}{4}\cdot\ldots\cdot\frac{k-1}{k}\cdot m_k(r) \tag{3}$$

Eq.3 is valid in the case of cylindrical symmetry.

3. FITTING OF THE SPATIAL MOMENTS

We need the following spatial moments as input data for our analytical model:

- mean projected range $R_p(E)$
- vertical standard deviation $\sigma_z(E)$
- vertical skewness $\gamma_z(E)$
- vertical kurtosis $\beta_z(E)$
- lateral standard deviation $\sigma_x(z,E)$
- lateral kurtosis $\beta_x(z,E)$

We have calculated these quantities by means of Monte Carlo method for 30 energies between 10 keV and 300 keV and in the case of lateral moments for approximately 40 intervalls of depth. To obtain small statistical fluctuations the simulation has been performed with 100,000 (boron) to 200,000 (antimony) ions. The results were then fitted by the below specified formulae.

3.1 Vertical moments

The vertical moments read

$$R_p(E) = a_1 \cdot E^{a2} + a_3 \tag{4a}$$

$$\sigma_z(E) = a_1 \cdot E^{a2} + a_3 \tag{4b}$$

$$\gamma_z(E) = \frac{a_1}{a_2+E} + a_3 \tag{4c}$$

$$\beta_z(E) = \frac{a_1}{a_2+E} + a_3 + a_4 \cdot E \ . \tag{4d}$$

The units used for the implantation energy E are keV, for all lengths (R_p, σ_z) μm are used. The parameters are listed in Table 1 to Table 4.

Table 1

Projected Range R_p

	boron	phosphorus	arsenic	antimony
a_1	0.00969	0.001555	0.000688	0.000668
a_2	0.767	0.958	0.983	0.921
a_3	-0.01815	0.000828	0.003962	0.005072
MSE	1.41 %	0.57 %	0.59 %	0.57 %

Table 2

Vertical Standard Deviation σ_z

	boron	phosphorus	arsenic	antimony
a_1	0.0521	0.002242	0.000402	0.000241
a_2	0.216	0.659	0.874	0.884
a_3	-0.0684	-0.003435	0.000582	0.000923
MSE	1.92 %	1.73 %	0.30 %	0.35 %

Table 3

Vertical Skewness γ_z

	boron	phosphorus	arsenic	antimony
a_1	312.7	336.2	339.8	195.1
a_2	122.2	199.3	342.0	339.7
a_3	-2.404	-1.386	-0.5051	-0.0910
MSE	0.0235	0.0093	0.0047	0.0068

Table 4

Vertical Kurtosis β_z

	boron	phosphorus	arsenic	antimony
a_1	0.	54.45	38.73	47.33
a_2	1.	55.74	61.70	81.17
a_3	2.212	1.865	2.559	2.692
a_4	0.0195	0.00482	0.	0.
MSE	1.66 %	0.39 %	0.60 %	0.58 %

MSE denotes the mean square error. Note that the fitting formulae are valid only in the range of 10 to 300 keV. We have tried to produce formulae that behave reasonable outside this range. Nevertheless R_p and σ_z do not approach 0 for implantation energy 0. Avoiding this would have resulted either in a considerable increase of the fitting error or in a more complex formula. So, if one insists on using our data for implantation energies less than 10 keV, one should rather interpolate R_p and σ_z linearly between 0 keV and 10 keV.

3.2 Lateral moments

Fitting two dimensional tables requires more complex formulae. We use:

$$\sigma_x(z,E) = \sigma_z(E) \cdot \{\frac{1}{a_1} \cdot \ln[\exp(a_1 \cdot P_1) + \exp(a_1 \cdot P_2)]\} \quad (5a)$$

$$\beta_x(z,E) = \frac{1}{a_1} \cdot \ln[\exp(a_1 \cdot P_1) + \exp(a_1 \cdot P_2)] \quad (5b)$$

with

$$P_1 = a_2 \cdot z' \cdot E + a_3 \cdot z' + a_4 \cdot E + a_5 \quad (6a)$$

$$P_2 = a_6 \cdot z' \cdot E + a_7 \cdot z' + a_8 \cdot E + a_9 \quad (6b)$$

and z' the reduced depth

$$z' = z/R_p(E) \ . \quad (6c)$$

The parameters a_1 - a_9 are listed in Table 5 and Table 6.

Table 5

Lateral Standard Deviation σ_x

	boron	phosphorus	arsenic	antimony
a_1	-1.443	-0.9488	-6.724	-13.884
a_2	-0.005637	0.002793	0.000582	0.000481
a_3	1.558	1.205	0.5117	0.3685
a_4	0.003511	-0.001370	-0.000649	-0.001024
a_5	1.189	1.043	0.3709	0.4838
a_6	-0.013185	-0.003208	-0.000512	-0.000110
a_7	-0.2271	-0.1201	0.1299	0.1357
a_8	0.014883	0.003528	0.000375	-0.000425
a_9	1.422	1.320	0.7277	0.7529

Table 6

Lateral Kurtosis β_x

	boron	phosphorus	arsenic	antimony
a_1	0.5278	0.03496	1.134	6.462
a_2	0.002498	-0.2996	-0.01340	-0.005668
a_3	-0.9765	-60.76	-2.927	-0.4474
a_4	-0.000061	0.008940	0.007873	0.004384
a_5	2.538	-53.66	4.493	3.345
a_6	0.02713	-0.001406	-0.000965	-0.000613
a_7	0.5976	0.2740	-0.06646	-0.11157
a_8	-0.03790	0.001470	0.001077	0.000901
a_9	0.5911	2.504	3.224	3.246

It is not reasonable to give a fitting error here because one could hardly decide if the error is due to fluctuations of the Monte Carlo results or to bad approximation. Instead, we have plotted the fitted and the unfitted moments in a three-dimensional representation. An example is shown in Fig.7 and Fig.8.

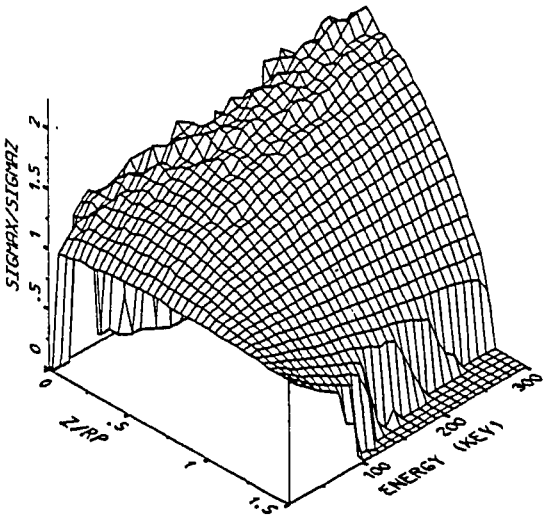

Fig.7: $\sigma_x(z,E)$ for boron (Monte-Carlo)

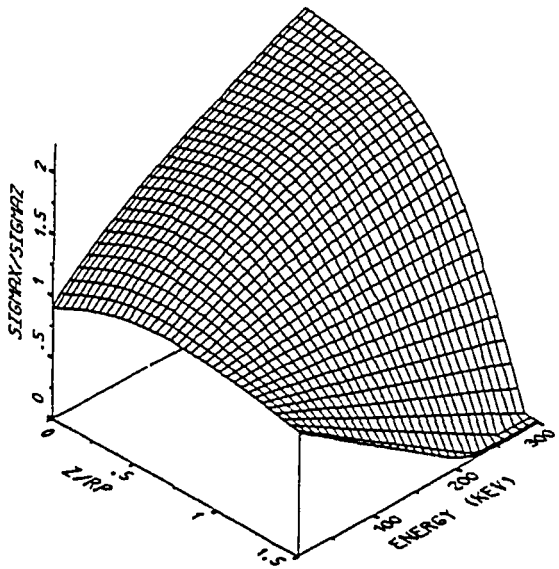

Fig.8: $\sigma_x(z,E)$ for boron (fitted)

4. ANALYTICAL MODEL

4.1 Vertical distribution function

We do not intend to present a new vertical distribution function here, but we want to point out a problem with the Pearson IV distribution, which arises together with moments derived from Monte Carlo calculations (it has already been encountered by Peterson et al. [10]): Skewness and kurtosis violate an inequality that restricts the applicability of the Pearson IV distribution. However, the Pearson IV function fits well experimental profiles in many cases [2]. The reason for this discrepancy is that real implantations are performed into crystalline targets where always a certain amount of channeling occurs.

There are various possibilities to overcome this problem. First, one can pragmatically modify the moments to meet the inequality between skewness and kurtosis (this has been done in Fig.3 to Fig.6). In most cases a slight modification is sufficient, so this will not cause a very great mistake. Then, another way is to perform a one-dimensional Monte Carlo simulation to obtain the vertical distribution function directly. This is in many cases feasible, because computer

time efficiency of Monte Carlo programs has increased considerably. The last possibility is to use an experimental profile for the vertical distribution. However, this method should be handled carefully, because if there is too much channeling in the profile, our data for the lateral standard deviation could possibly not apply.

4.2 Lateral distribution function

We look for a function $f(x)$ with the following characteristics:

- symmetry
- positivity
- only one maximum
- smoothness
- its parameters can be calculated from standard deviation σ and kurtosis β. For that purpose the moments must exist to the forth order.

The function $f(x)$ has to meet the equations

$$1 = \int_{-\infty}^{\infty} f(x)\, dx \tag{7a}$$

$$\sigma^2 = \int_{-\infty}^{\infty} x^2 \cdot f(x)\, dx \tag{7b}$$

$$\beta \cdot \sigma^4 = \int_{-\infty}^{\infty} x^4 \cdot f(x)\, dx\ . \tag{7c}$$

Thus we need (at least) 3 free parameters. The Gaussian function

$$f(x) = a \cdot \exp(-(bx)^2) \tag{8}$$

has only two parameters, which are determined by Eq.7a and Eq.7b:

$$a = \frac{1}{\sqrt{2\pi} \cdot \sigma} \tag{9a}$$

$$b = \frac{1}{\sqrt{2} \cdot \sigma} \tag{9b}$$

The kurtosis equals 3 in any case. In order to obtain one additional parameter, we replace the power 2 in the Gaussian function (8) by an arbitrary power p:

$$f(x) = a \cdot \exp(-|bx|^p) \tag{10}$$

Introducing (10) into (7), we need the integral [11]

$$\int_0^\infty x^n \cdot \exp(-|bx|^p)\, dx = \Gamma\left(\frac{n+1}{p}\right) / \left(p \cdot b^{n+1}\right) . \qquad (11)$$

Γ denotes the Gamma function. β can be expressed, using Eq.7:

$$\beta = \frac{\Gamma\left(\frac{1}{p}\right) \cdot \Gamma\left(\frac{5}{p}\right)}{\Gamma\left(\frac{3}{p}\right)^2} \qquad (12)$$

We need the inverse function of (12), what unfortunately cannot be done analytically. So we solved the problem for very large p:

$$\left(\frac{1}{p}\right)_o = 0.290576 \cdot \sqrt{\beta - 1.8} \qquad (13a)$$

and for very small p:

$$\left(\frac{1}{p}\right)_\infty = 0.687042 \cdot \ln\left(\frac{\sqrt{5} \cdot \beta}{3}\right) \qquad (13b)$$

The actual value of $\frac{1}{p}$ is obtained by interpolation

$$\frac{1}{p} = c \cdot \left(\frac{1}{p}\right)_o + (1-c) \cdot \left(\frac{1}{p}\right)_\infty \qquad (13c)$$

with

$$c = 0.795833 \cdot \exp[-1.94544 \cdot (\beta - 1.8)] + 0.204167 \cdot \exp[-0.272172 \cdot (\beta - 1.8)] . \qquad (13d)$$

(13d) was fitted to 100 (β,p)-values in the range $1.8 < \beta < 6$. The mean square error is about 1 %, but it is centered at very small β, so the error in the relevant range of β is less (e.g. β=3 leads to p=1.999 instead of 2, which is correlated by Eq.12 to β=3.001).

With p from (13c) one obtains easily

$$b = \frac{1}{\sigma} \cdot \sqrt{\Gamma\left(\frac{3}{p}\right) / \Gamma\left(\frac{1}{p}\right)} \qquad (14)$$

and

$$a = (b \cdot p) / \left(2 \cdot \Gamma\left(\frac{1}{p}\right)\right) . \qquad (15)$$

Eq.10 is shown in Fig.9 for various values of β. For β=6 (p=1) the derivation of f(x) at x=0 is discontinuous and for $\beta > 6$ it becomes infinite. However, in the case of ion implantation lateral kurtoses greater than 6 do practically not appear.

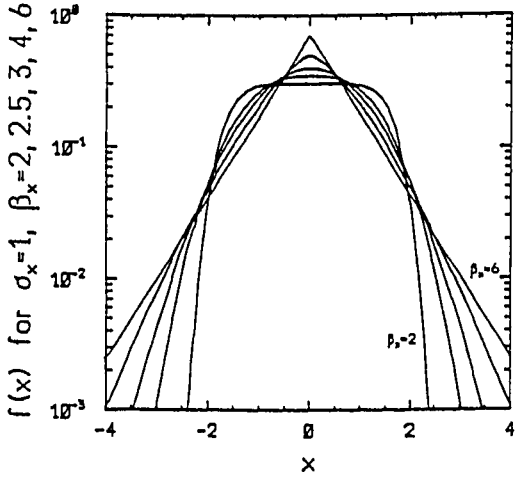

Fig.9: Eq.10 for various values of β

4.3 Distribution under a mask edge

Seeing σ and β as functions of z ($\sigma_x(z,E)$, $\beta_x(z,E)$), f(x) of the previous section may be called $f_{lat}(x,z)$. Multiplication with the vertical distribution function $f_{vert}(z)$ yields the two-dimensional distribution function for one ion (cf. Eq.2). This distribution function can then be used in a convolution integral to calculate the distribution function under a mask edge [4], [5], [6]. We do not discuss the convolution integral, but we note that it does not treat those ions correctly which leave the mask into the air and reenter the target.

The results of our calculations for an infinitely steep mask edge are shown in Fig.5 and Fig.6. In both cases the vertical distribution function has been assumed a Pearson IV function. The vertical kurtosis has been modified as mentioned in Section 4.1. In Fig.5 the lateral kurtosis has been assumed β=3, so we have a Gaussian distribution laterally, but with a depth dependend standard deviation. In Fig.6 we also account for the lateral kurtosis.

ACKNOWLEDGEMENT

This work was supported by the research laboratories of SIEMENS AG at Munich, FRG.

5. REFERENCES

1. LINDHARD, J., SCHARFF, M. and SCHIØTT, H.E.
"Range Concepts and Heavy Ion Ranges"
Mat. Fys. Medd. Dan. Vid. Selsk. Vol. 33, No. 14, 1963.

2. RYSSEL, H. and BIERSACK, J.P.
"Ion Implantation Models for Process Simulation", In:
Process and Device Modeling (Ed. W.L. Engl), Elsevier
Science Publishers B.V., North Holland, p.31, 1986.

3. HOFKER, W.K.
"Concentration Profiles of Boron Implantations in
Amorphous and Polycrystalline Silicon"
Philips Research Rep. Vol. Suppl., p.41, 1975.

4. FURUKAWA, S., MATSUMURA, H. and ISHIWARA, H.
"Theoretical Considerations on Lateral Spread of Implanted
Ions"
Jap. J. Appl. Phys. Vol. 11, No. 2, p.134, 1972.

5. RUNGE, H.
"Distribution of Implanted Ions under Arbitrarily Shaped
Mask Edges"
Phys. Stat. Sol. (a) Vol. 39, p.595, 1977.

6. SELBERHERR, S.
"Analysis and Simulation of Semiconductor Devices"
Springer, Wien-New York, 1984.

7. RYSSEL, H.
"Implantation and Diffusion Models for Process Simulation"
Proc. VLSI Process and Device Modeling, Katholieke
Universiteit Leuven, p.1, 1983.

8. BIERSACK, J.P. and HAGGMARK, L.G.
"A Monte Carlo Computer Program for the Transport of
Energetic Ions in Amorphous Targets"
Nucl. Inst. Meth. Vol. 174, p.257, 1980.

9. ZIEGLER, J.F., BIERSACK, J.P. and LITTMARK, U.
"The Stopping and Range of Ions in Solids"
Pergamon Press, New York, 1985.

10. PETERSON, W.P., FICHTNER, W. and GROSSE, E.H.
"Vectorized Monte Carlo Calculations for the Transport of
Ions in Amorphous Targets"
IEEE Trans. Electron Dev. Vol. ED-30, No.9, p.1011, 1983.

11. GRADSHTEYN, I.S. and RYZHIK, I.M.
"Table of Integrals, Series, and Products. Corrected and
Enlarged Edition", p.342
Academic Press, New York, 1980.